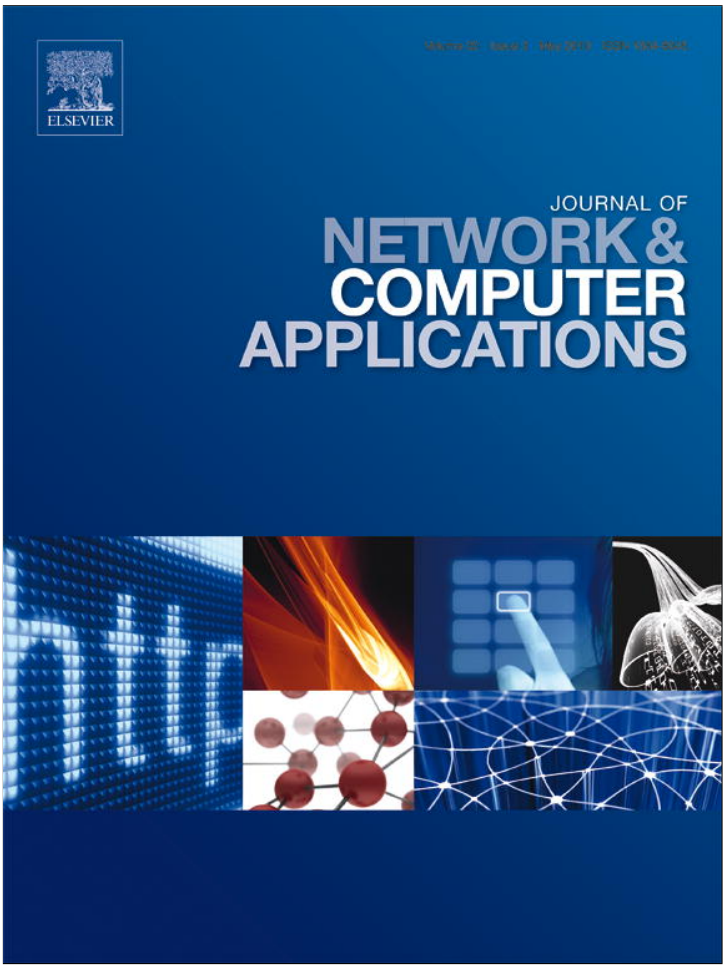

Journal of Network and Computer Applications 33 (2010) 258–267

Contents lists available at ScienceDirect

Journal of Network and Computer Applications

journal homepage: www.elsevier.com/locate/jnca

Combining features for distorted fingerprint matching

Kai Cao [1], Xin Yang [1], Xunqiang Tao, Peng Li, Yali Zang, Jie Tian *

Institute of Automation, Chinese Academy of Sciences, Beijing 100190, China

ARTICLE INFO

Article history:
Received 30 July 2009
Received in revised form
14 November 2009
Accepted 7 December 2009

Keywords:
Distorted fingerprint matching
Ridge compatibility
Local feature
Finger placement direction

ABSTRACT

Extracting and fusing discriminative features in fingerprint matching, especially in distorted fingerprint matching, is a challenging task. In this paper, we introduce two novel features to deal with nonlinear distortion in fingerprints. One is finger placement direction which is extracted from fingerprint foreground and the other is ridge compatibility which is determined by the singular values of the affine matrix estimated by some matched minutiae and their associated ridges. Both of them are fixed-length and easy to be incorporated into matching score. In order to improve the matching performance, we combine these two features with orientation descriptor and local minutiae structure, which are used to measure minutiae similarity, to achieve fingerprint matching. In addition, we represent minutiae set as a graph and use graph connect component and iterative robust least square (IRLS) to detect creases and remove spurious minutiae close to creases. Experimental results on FVC2004 DB1 and DB3 demonstrate that the proposed algorithm could obtain promising results. The equal error rates (EER) are 3.35% and 1.49% on DB1 and DB3, respectively.

1. Introduction

Fingerprints are graphical patterns of ridges and valleys on the skin surface of fingertips (Maltoni et al., 2009), and the uniqueness of a fingerprint can be determined by the overall pattern of ridges and valleys as well as the local ridge minutiae (ridge ending and ridge bifurcation). Fingerprint recognition has been studied for many years and lots of algorithms have been proposed to improve the performance of automatic fingerprint identification system (AFIS). Minutiae-based matching algorithms are the most popular approaches to fingerprint recognition since it is widely believed that minutiae are the most discriminating and reliable features. Given two minutiae sets, minutiae matching is a complex combinatorial problem, because two fingerprints may be translated, rotated and especially nonlinear distorted with respect to each other, and both minutiae sets may suffer from false, missed, and displaced minutiae. Many researchers have tried to exploit assistant features to reduce the ambiguity between minutiae. Typical assistant features include ridge feature, local minutiae structure and local orientation feature.

Ridge feature is the first local feature introduced in fingerprint matching (Jain et al., 1997). Jain et al. (1997) utilized ridge information as an aid for alignment. In this method, for each minutiae pair (one from the input fingerprint, the other one from the template fingerprint), if their associated ridges were similar the input minutiae set was rotated and translated based on this minutiae pair. Minor modifications of this algorithm have been proposed to establish minutiae correspondence and reduce the computational cost (He et al., 2003; Luo et al., 2000). He et al. (2006) proposed a global comprehensive similarity-based fingerprint matching algorithm, in which minutia-simplex, including a pair of minutiae as well as their associated ridges, was employed to ensure positional constraint. This method obtained a good trade-off between matching performance and computational expense. Wang et al. (2007) proposed a feature called PolyLines to extract ridge information. Three transformation-invariant features were calculated for each ridge sampling point and ridge similarity was based on these features. However, all the features above seem not excellent in case of severe distortion. Ridge counts among matched minutiae pairs (Sha et al., 2006) are high discriminating feature and robust to distortion, but they are difficult to reliably extract in the presence of noise, and then are rarely used in automated systems (Yager and Amin, 2004).

Local minutiae structure, which consists of neighboring minutiae, is one of the most discriminative features used in fingerprint matching. Jiang and Yau (2000) and Jea and Govindaraju (2005) utilized k closest neighboring minutiae points to generate a fixed-length local minutiae feature for each minutia and the similarities between minutiae were based on these features. An advantage of the fixed-length feature is that the similarity between two feature vectors can be computed very fast. But it is sensitive to the order of the neighboring minutiae. Ratha

* Corresponding author. Tel.: +86 10 826 184 65; fax: +86 10 625 279 95.
E-mail address: tian@ieee.org (J. Tian).
URL: http://www.fingerpass.net (J. Tian).
[1] These authors contribute equally to this work.

1084-8045/$ - see front matter © 2009 Elsevier Ltd. All rights reserved.
doi:10.1016/j.jnca.2009.12.007

et al. (2000) and Chen et al. (2006) adopted similar strategies by defining a feature vector which characterized the rotation and translation invariant relationship between a minutia and its neighbors circled within a radius. Feng (2008) extended this approach by transforming the input minutiae structure to deal with the occlusion problem and giving a specific formula to measure the similarity between two minutiae structures. Cao et al. (2009) modified this formula by taking the position and direction of the neighboring minutiae into account to make the minutiae structure similarity measure more accurate.

Orientation feature, which characterizes the ridge flow in fingerprints, is one of the fundamental statistical feature. It plays an important role in automatic fingerprint identification system (AFIS) process, since it is essential for not only fingerprint enhancement (Hong et al., 1998) but also fingerprint pattern classification (Maio and Maltoni, 1996) and fingerprint matching. The approaches presented in Tico and Kuosmanen (2003) and Tong et al. (2005) built transformation-invariant orientation feature vectors, which comprised the orientation distances of the sampling points surrounding a minutia and the minutia itself. The difference between them is the sampling strategy. Wang et al. (2007) proposed a feature called OrientationCodes, in which the ROI was circularly tessellated through several bands and sectors, and the orientation was estimated by least square error. Gu et al. (2006) and Qi et al. (2005) viewed the orientation field as a global feature and combined it with minutiae to match fingerprints.

However, there are still difficulties in fingerprint matching. Local features, such as orientation descriptor and local minutiae structure, are less sensitive to nonlinear distortion which is small in local region. Adding more local features can reinforce the individuality of fingerprints. However, fingerprints from different fingers may possess similar minutiae, orientation and ridge features in the overlapped region. Fig. 1 shows an example of a pair of fingerprints from FVC2004 DB3. In Fig. 1(c) the minutiae in the overlapped region possess similar local features. In this paper we proposed a novel feature called finger displacement direction which is extracted from fingerprint foreground to reduce the false matching resulted from similar local feature.

Ridges are easily interrupted by noise and local deformation will distort the ridge shapes largely. The length of a ridge may vary in different fingerprints and long ridge has larger variation than short ridge. Therefore, it is hard to select parameters to measure the similarity between ridges. And conventional ridge feature is hard to improve distorted fingerprint matching. A novel feature called ridge compatibility is proposed to deal with this problem. Different from convectional method, ridge compatibility is calculated by the singular values of the affine matrixes, which are estimated by pairwise ridge sampling points associated with matched minutiae.

In addition, we propose a graph-based algorithm to remove spurious minutiae resulted from creases since spurious minutiae degrade heavily the performance of fingerprint matching algorithms (as shown in Fig. 2). Then we combine the proposed two novel features with orientation descriptor and local minutiae structure to improve the matching performance. Experimental results on FVC2004 DB1 and DB3, in which the distortion between some fingerprints from the same finger is large, indicate that the proposed algorithm obtains promising results. The equal error rates (EER) are 3.35% and 1.49% on DB1 and DB3, respectively. Both of them can obtain the third place in FVC2004 ranked by EER.

The rest of the paper is organized as follows: Section 2 gives feature extraction and fingerprint representation. Section 3 presents the minutiae similarity calculation, minutiae pairing and matching score computation. The experimental results are reported in Section 4 and conclusions are drawn in Section 5.

2. Feature extraction

In this section, we will present the strategy to remove spurious minutiae close to creases and extract the features used by the matching algorithm. The orientation field of a gray-scale fingerprint image is computed by the approach proposed by Bazen and Gerez (2002). Foreground of fingerprint image is segmented by the approach in Chen et al. (2004). Then the method proposed by Hong et al. (1998) is used to enhance the image and obtain the thinned ridge map. Minutiae set $M=\{m_i=(x_i,y_i,\theta_i)\}_{i=1}^{n}$ is detected by Hong et al.'s (1998) method, where n denotes the number of detected minutiae, x_i y_i and θ_i denote the x coordinate, y coordinate and the direction of minutia m_i, respectively.

2.1. Spurious minutiae removing

From Fig. 2, we can obtain that the spurious minutiae resulted from a crease have the following characters: (i) The spurious minutiae from the same side of a crease possess similar direction. They are approximately distributed on a line and the distance between two neighboring minutiae is approximately equal to the ridge width. (ii) The nearest two spurious minutiae from different sides of a crease have nearly opposite directions, and the distance between them is approximately equal to the width of the crease.

Fig. 1. An example of two fingerprints with similar local feature but different finger placement direction. (a) Skeleton image of 38_1.tif from FVC2004 DB3, (b) skeleton image of 89_1.tif from FVC2004 DB3, (c) registration of (a) and (b).

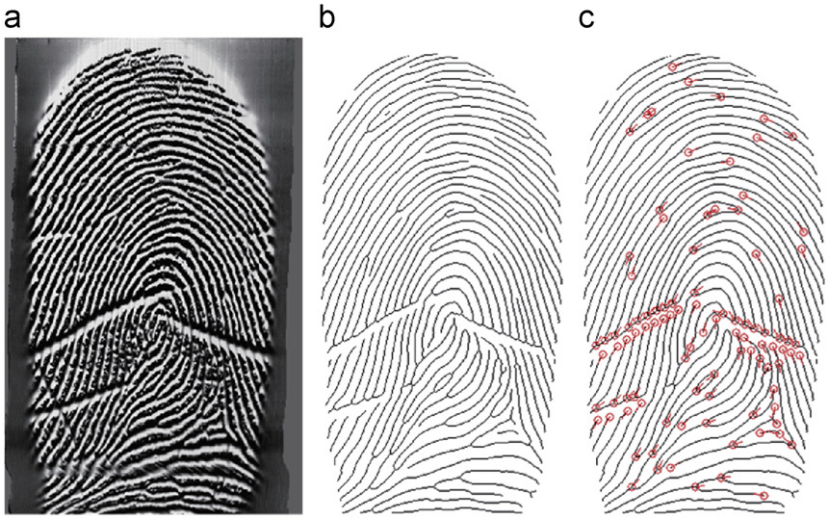

Fig. 2. An example of a fingerprint with creases. (a) Original fingerprint (FVC2004 DB3 100_1.tif), (b) skeleton image of (a), (c) the minutiae with their direction given on the skeleton image.

Based on these two observations we propose a graph-based approach to remove the spurious minutiae close to the creases. The detailed procedure is described as follows:

Step 1: An undirected graph $G=(V,E)$ is constructed by the minutiae set M. The vertex set V of the graph G consists of all the minutiae. The edge attribute $e_{ij}\in\{0,1\}$ is binary, denoting the absence or presence of an edge. If $e_{ij}=1$, it means that there is an edge connecting the i th and the j th minutia, which satisfy one of the following conditions :

$$dLen(m_i,m_j)<D_{Thr1} \quad \text{and} \quad |d\theta(\theta_i,\theta_j)|<\theta_{Thr1}, \tag{1}$$

$$dLen(m_i,m_j)<D_{Thr2} \quad \text{and} \quad |d\theta(\theta_i,\theta_j)|>\pi-\theta_{Thr2}, \tag{2}$$

where $D_{Thr1}, D_{Thr2}, \theta_{Thr1}$ and θ_{Thr2} are thresholds, $dLen(m_i,m_j)$ is Euclid distance defined in Eq. (3) and $d\theta(\theta_1,\theta_2)$ is directional distance function defined in Eq. (4):

$$dLen(m_i,m_j)=\sqrt{(x_i-x_j)^2+(y_i-y_j)^2}, \tag{3}$$

$$d\theta(\theta_1,\theta_2)=\begin{cases}\theta_1-\theta_2 & \text{if } |\theta_1-\theta_2|\le\pi,\\ \theta_1-\theta_2-2\pi & \text{if } (\theta_1-\theta_2)>\pi,\\ \theta_1-\theta_2+2\pi & \text{otherwise.}\end{cases} \tag{4}$$

Step 2: A crease usually results in many spurious minutiae. And for each of them, it is probable that there exists a minutiae adjacent to it. Therefore, based on the graph representation in Step 1 minutiae which are close to a crease are expected to be connected. The disjoint-set data structures (Cormen et al., 2001) is adopted to determine the connected components of the undirected graph G. A connected component in which there are more than N_s vertices ($N_s=7$ in our experiments) is supposed to be close to a crease and then it is referred to as a crease component. Fig. 3(a) marks the three crease components.

Step 3: Since the spurious minutiae resulted from a crease are expected to line up along the crease, we use a line to model the crease. For each crease component C, the line parameters are expected to minimize the following objective function:

$$E(C,a,b)=\sum_{m_i\in C}\rho((y_i-a\cdot x_i-b)/\sigma), \tag{5}$$

where a is the slope of the line, b is the intercept, $\rho(u)$ is a robust loss function, monotonically nondecreasing as a function of u, and σ is the error scale. Function (5) is minimized using IRLS (Holland and Welsch, 1977), with weight function $w(u)=\rho'(u)/u$. In this paper, we choose Beaton–Tukey biweight function (Holland and Welsch, 1977) as the objective function. In detail, the weight function is

$$w(u)=\begin{cases}\left[1-\left(\frac{u}{4}\right)^2\right]^2, & |u|\le 4,\\ 0, & |u|>4.\end{cases} \tag{6}$$

Fig. 3(b) gives three estimated lines.

Step 4: If the number of the minutiae which belong to the crease component and close to the line is still larger than N_s, these minutiae close to the line are deemed to be spurious and removed from the minutiae set. Fig. 3(c) illustrates the minutiae with their direction after removing spurious minutiae.

It is difficult to reliably extract minutiae from the input fingerprint, especially from the low quality fingerprint images. Therefore, the method proposed by Feng (2008) is used to classify a minutia as reliable or unreliable one, which is used in minutiae similarity estimation and matching score computation.

2.2. Global feature extraction

In this section, we present an approach to extract finger placement direction. For most fingerprints, we can judge the finger placement (including position and direction) by its overall ridge pattern. However, it is hard to extract a feature related with the finger placement direction from the ridge pattern. When touching the finger tip against the plain surface of an acquisition sensor or sweeping it against the narrow stripe, the three-dimensional elastic surface of a finger is projected to generate a flat fingerprint image. This process introduces nonlinear distortions that ridge pattern may be warped largely. However, the acquired fingerprint seems to be a long shape no matter where the direction of the force is, because a finger can be viewed as a long cylinder. Therefore, ridge distortion has little influence on the finger displacement direction.

Hence we try to directly extract finger displacement direction from the shape of the fingerprint. The method described in Freeman and Shapira (1975) is modified to achieve this task. We shall proceed in three steps. First, the border of fingerprint foreground is sampled and represented as a plane curve. Then, Graham's, 1972 algorithm, which is an important sequential algorithm used for determining the convex hull of a point set in the plane, is adopted to determine its minimum-perimeter convex

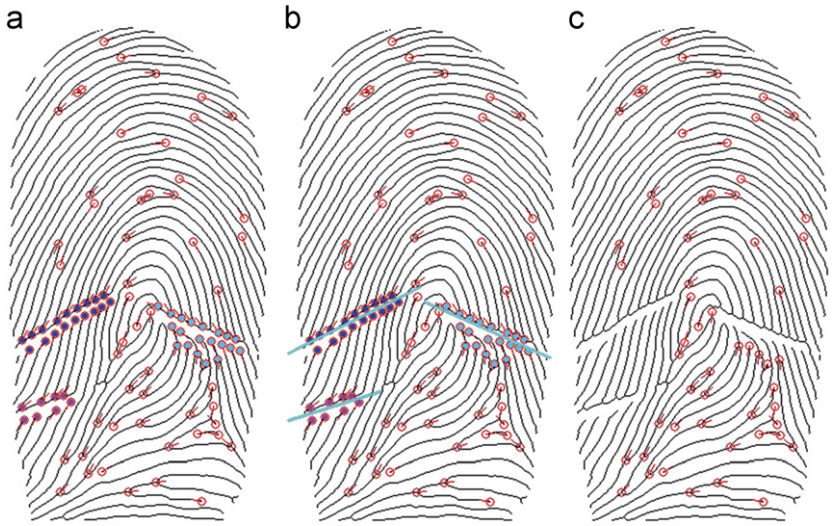

Fig. 3. Illustration of spurious minutiae removing: (a)connected component of the minutiae graph, (b) detected creases, (c) minutiae with their direction after spurious minutiae removing.

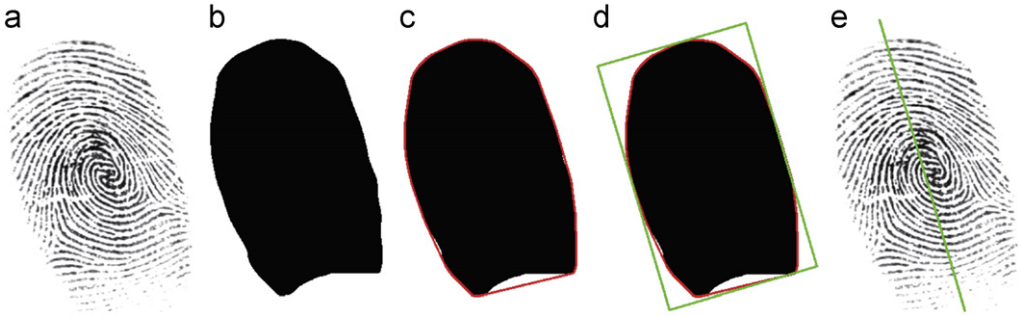

Fig. 4. Illustration of finger placement direction extraction, (a) original fingerprint (1_6.tif from FVC2004 DB1), (b) foreground of (a), (c) convex hull of (b), (d) the minimum-area encasing rectangle for (c), (e) fingerprint with finger placement direction.

polygon that encases the given plane curve (i.e. convex hull). Finally, it is only necessary to test the set of rectangles having one side collinear with the polygon's edges for the rectangle with least area, and the minimum-area rectangle that encases this convex polygon is selected. Since a finger is generally placed upward, the upward direction of the longer side of the rectangle is deemed as the finger placement direction. Fig. 4 illustrates the extraction process. To extract robust and accurate feature, finger placement direction can be defined only when the rectangle satisfies the condition that the length of the rectangle should be larger than 1.2 times of the width. Fig. 5 gives an instance that does not satisfy this condition.

3. Fingerprint matching

3.1. Minutiae similarity

Local features of a minutia describe the characteristics in its neighborhood and are less sensitive to nonlinear distortion. They can be used to find potential matches in another minutiae set and calculate matching score. In this section, we combine orientation descriptor and local minutiae structure to measure the similarity between minutiae.

The local orientation-based descriptor proposed by Tico and Kuosmanen (2003) is invariant to rotation and translation and it has been reported to have better performance than previous ones. The descriptor comprises the orientation information at some sampling points around the minutiae point in a circular pattern. The circular pattern consists of L concentric circles of radii r_l $(1 \le l \le L)$ and K_l sampling points are equally sampled on the l th circle. The minutiae descriptor is invariant to rotation and translation. In this paper, the parameters suggested by Tico and Kuosmanen (2003) is adopted, which is $((r_0 = 27, K_0 = 10), (r_1 = 45, K_1 = 16), (r_2 = 63, K_2 = 22), (r_3 = 81, K_3 = 28))$. Let $p = \{\alpha_{k,l}\}$ and $q = \{\beta_{k,l}\}$ be two minutia descriptors. Here, we also use p and q to represent corresponding minutiae, without risk of ambiguity. The orientation descriptor similarity (OS) between p and q is computed as

$$OS_{pq} = 1/K \sum_{l=1}^{L} \sum_{k=1}^{K_l} s(\Lambda(\alpha_{k,l}, \beta_{k,l})), \tag{7}$$

where $\Lambda(\theta_1, \theta_2)$ is the orientation distance between θ_1 and θ_2, and $s(x)$ denotes a similarity value with respect to the angle.

Local minutiae structural similarity in this section is measured by our previous work (Cao et al., 2009). For the completeness, we describe the process in brief. Suppose p is a minutia in the template fingerprint and q is a minutia in the input fingerprint, the similarity calculation process can be divided into two stages: (1) minutia p and its neighbors are mapped to the coordinate system of q, (2) minutia q and its neighbors are mapped to the coordinate system of p. In order to deal with the distortion, the

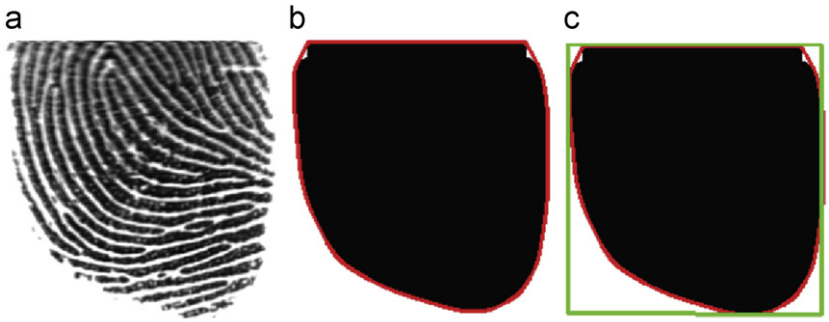

Fig. 5. An example that its finger placement direction cannot be extracted. (a) original fingerprint (17_1.tif from FVC2004 DB1), (b) foreground of fingerprint and its convex hull, (c) the minimum-area encasing rectangle for (b).

neighboring radius of the target minutia should be larger than that of the mapped minutia.

In the stage (1), let $N(p,r)=\{p_i\}_{i=1}^{n_p}$ denote the set of the neighboring minutiae circled p within r radius, $N(q,r+\Delta r)=\{q_j\}_{j=1}^{n_q}$ denote the set of the neighboring minutiae circled q within $r+\Delta r$ radius and T represent the corresponding rigid transformation from p to q . Each minutia p_i in $N(p,r)$ is mapped to p_i' using T. Then the contribution of p_i' with respect to the minutia p is computed as

$$C_{p_i}=\max_{q_j} f(dLen(p_i',q_j),Len_1,Len_2)\cdot f(d\theta(p_i',q_j),\theta_1,\theta_2) \tag{8}$$

where Len_1 and Len_2 are two distance thresholds, θ_1 and θ_2 are two direction distance thresholds, and the function f is defined as

$$f(x,th1,th2)=\begin{cases}1 & \text{if } x\le th1,\\ 0 & \text{if } x>th2,\\ \dfrac{x-th1}{th2-th1} & \text{otherwise.}\end{cases} \tag{9}$$

If C_{p_i} is lager than 0, p_i is regarded as a matching minutia.

In the stage (2), we define another two neighboring structures: $N(q,r)$ and $N(p,r+\Delta r)$, the meaning of which is similar as stage 1. We use the same symbol T to represent the relative rigid transformation from q to p. Each minutia $q_j\in N(q,r)$ is mapped to q_j' using T. The contribution of q_j to the minutia q is calculated as follows:

$$C_{q_j}=\max_{p_i} f(dLen(p_i,q_j'),Len_1,Len_2)\cdot f(d\theta(p_i,q_j'),\theta_1,\theta_2). \tag{10}$$

The similarity based on local minutiae structure between p and q is measured using the following formula:

$$MS_{pq}=\frac{1+\sum_{p_i\in N(p,r)}C_{p_i}}{M_p+bias}\cdot\frac{1+\sum_{q_j\in N(q,r)}C_{q_j}}{M_q+bias}, \tag{11}$$

where M_p and M_q represent the number of minutiae of $N(p,r)$ and $N(q,r)$ that should be matched (Feng, 2008) and *bias* is a parameter. Minutia m is regarded as a minutia that should be matched, if m' is a matched minutia or it is a reliable minutia on the foreground of the other fingerprint.

The similarity based on local minutiae structure captures local minutiae pattern while orientation descriptor captures local ridge flow. Therefore, these two features are independent with each other. Two similarity functions are combined to measure the similarity between the minutiae pair by product rule:

$$S_{pq}=OS_{pq}\cdot MS_{pq}. \tag{12}$$

3.2. Minutiae pairing

Let $\{p_k\}_{k=1}^{N_I}$ and $\{q_l\}_{l=1}^{N_T}$ denote two minutiae sets from input and template fingerprint, respectively, and $s=\{S_{kl}\}_{k=1,l=1}^{N_I,N_T}$ denote the set of similarity degrees between two minutiae sets. However, a minutia may exhibit a large similarity degree with more than one minutia. To determine the order in which to insert correspondences, the similarity degree set s is normalized by the method proposed by Feng (2008), formally,

$$NS_{pq}=\frac{S_{pq}\cdot(N_T+N_I-1)}{\sum_{k=1}^{N_I}S_{kq}+\sum_{k=1}^{N_T}S_{pk}-S_{pq}}. \tag{13}$$

Then minutiae pairs are sorted in decreasing order of *NS* and the top K minutia pairs are used as the reference pair candidates. For each of them, a matching attempt is performed: (1) two fingerprints are aligned using the relative translation and rotation between the reference pair; (2) the greedy matching algorithm proposed by Feng (2008) is used to establish the correspondences between two minutiae sets; (3) then the score of this attempt is calculated based on the correspondences. The maximal score of these attempts is selected as the matching score.

3.3. Matching score computation

A conventional way to calculate matching score for a minutiae point pattern matching system is based on the following formula (Jain et al., 1997):

$$score=n^2/(N_I\times N_T), \tag{14}$$

where N_I and N_T represent the numbers of minutiae in input and template minutiae sets, respectively, and n is the number of matched minutiae in both sets. Bazen and Gerez (2003) claimed that using $2n/(N_t+N_q)$ to compute matching score will give better results. However, both of these two types cannot deal with low-quality fingerprint images and small overlap region. To solve these problems, Tico and Kuosmanen (2003) modified the formula (14) by replacing the number of matched minutiae with the total similarity of orientation descriptor between matched minutiae set and replacing the numbers of minutiae in two fingerprints with the numbers of minutiae in the common region. Sheng et al. (2007) proposed to use the following matching rate score:

$$score=\frac{2\sum_{k=1}^{n}S_{p_kq_k}}{SN_I+SN_T}, \tag{15}$$

where $\{(p_k,q_k)\}_{k=1}^{n}$ is the matched minutiae pair set, SN_I and SN_T are the number of minutiae that should be matched for input and template fingerprints, respectively. However, we think all the measures are not accurate enough. In this section, we try to incorporate fingerprint placement direction and ridge compatibility into the matching score computation in order to improve the algorithm performance.

3.3.1. Global feature similarity

Suppose that the finger placement directions are θ_I and θ_T for input and template fingerprints, respectively. For each matched

minutiae pair (p_k, q_k), the directional distances (β_k^1, β_k^2) between the minutia direction and its corresponding finger placement direction are utilized to describe the matching status, where $\beta_k^1 = d\theta(\theta_{p_k}, \theta_I)$ and $\beta_k^2 = d\theta(\theta_{q_k}, \theta_T)$. Let $\beta_k = |d\theta(\beta_k^1, \beta_k^2)|$ denote the matching difference between the k th matched minutiae pair. Then the average of the matching differences is estimated as

$$\beta_{diff} = \frac{1}{n}\sum_{k=1}^{n} \beta_k. \tag{16}$$

In the case that one of the compared fingerprints does not have finger placement direction, the value of β_{diff} is set as zero. This is because we cannot calculate its global similarity and assume that the global features are perfectly matched. The global similarity is calculated as follows:

$$S_g = f(\beta_{diff}, \beta_{Thr_1}, \beta_{Thr_2}), \tag{17}$$

where f is the fuzzy membership function given in Eq. (9), β_{Thr_1} and β_{Thr_2} are two thresholds.

3.3.2. Ridge compatibility

Another feature incorporated into the matching score is the ridge information. Once the minutiae correspondences are established, their associated ridges are established too. However, ridges are easily impacted by noise, dir, nonlinear distortion and so on. Therefore, it is hard to determine the parameters used in conventional ridge similarity function. In this section, we propose a feature, called ridge compatibility, based on singular value decomposition (SVD) to measure the ridge similarity. Using the minutiae pairing algorithm stated in Section 3.2, the matched minutiae pairs between input and template fingerprints can be obtained. The corresponding sampling points are considered to be matched if their associated minutiae are matched. If the number of sampling points for one minutia in a pair is different from the second minutia of the pair, we set the smaller number as the number of matched sampling points (Chen et al., 2006). Note that the first sampling point of each ridge refers to the minutia, and the ridge corresponding to a bifurcation serves as a virtual ridge in the middle of two nearest ridges surrounding the direction of the bifurcation (Wang et al., 2007). Suppose that $P_I = (x_i, y_i)_{i=0}^{n_s}$ is a ridge sampling point set in input fingerprint, $P_T = (u_i, v_i)_{i=0}^{n_s}$ is the matched ridge sampling point set in template fingerprint and n_s is the number of matched ridge sampling points. The affine model is adopted to model the transformation between two point sets. The affine transformation of a input point $X_i = (x_i, y_i)^T$ to a template point $Y_i = (u_i, v_i)^T$ can be written as

$$Y_i = A \cdot X_i + t, \tag{18}$$

where t is 2×1 translation vector, and A is a 2×2 transformation matrix which denotes the affine rotation, scale, and shearing. These parameters are supposed to minimize the following objective function:

$$Obj(A, t) = \frac{1}{n_s}\sum_{i=1}^{n_s} \|A \cdot X_i + t - Y_i\|, \tag{19}$$

where n_s is the number of the sampling points. Based on singular value decomposition (SVD), the matrix A can be decomposed as follows:

$$A = U \cdot \Lambda \cdot V^T = \begin{bmatrix} \cos(\varphi) & \sin(\varphi) \\ -\sin(\varphi) & \cos(\varphi) \end{bmatrix} \cdot \begin{bmatrix} \lambda_1 & 0 \\ 0 & \lambda_2 \end{bmatrix} \cdot \begin{bmatrix} \cos(\theta) & -\sin(\theta) \\ \sin(\theta) & \cos(\theta) \end{bmatrix}, \tag{20}$$

where λ_1 and λ_2 are the singular values of A, U and V are 2×2 unitary matrices, φ and θ are angles related to U and V. From the decomposition it is easy to see that U and V are only related with rotation while the singular values are related with the scale transformation. Therefore, the singular values are expected to close to 1 for genuine matches. In order to balance the efficiency and matching accuracy, we select two matched minutiae pairs ((q_i, p_i) and (q_j, p_j)) and their associated ridge sampling points to estimate the affine matrix A_{ij} and calculate corresponding singular values ($\lambda_{ij,1}$ and $\lambda_{ij,2}$) each time. Then, we define the ridge compatibility (RC) by the singular values, formally,

$$RC = \frac{2}{n(n-1)}\sum_{i=1}^{n}\sum_{j=i+1}^{n} ((\lambda_{ij,1}-1)^2 + (\lambda_{ij,2}-1)^2). \tag{21}$$

The similarity based on ridges (S_r) are calculated as follows:

$$S_r = \exp\left(-\frac{RC}{\sigma^2}\right), \tag{22}$$

where σ is a parameter which controls the width of the "bell" curve.

In order to achieve the better classification performance, the three parts are combined by product rule to give the matching score. Note that in order to reduce false acceptance rate (FAR), the matching score is set as zero if matched minutiae number is less than 4.

4. Experimental results

Since our work is to deal with the problem of distorted fingerprint matching, the evaluation of the proposed algorithm is conducted on FVC2004 (2004) DB1 and DB3, in which, the distortion between some fingerprints from the same finger is obvious. In this section, two sets of experiments are conducted to evaluate spurious minutiae removing and the overall performance of the proposed algorithm. The performance evaluation protocol used in FVC2002 (2002) has been adopted. Each sample is matched against the remaining samples of the same finger in genuine match. In imposter match, the first sample of each finger is matched against the first sample of the remaining fingers. Hence, there are total 2800 genuine tests and 4950 imposter tests in each database.

4.1. Spurious minutiae removing

An experiment is conducted on FVC2004 DB3 to evaluate the validity of the spurious minutiae removing process. The matching score is calculated by using Eq. (15). Fig. 6 shows the receiver operating curves (ROCs) plotting FMR vs. FNMR of the algorithm without removing spurious minutiae and the algorithm with removing spurious minutiae. The performance indices (EER, FMR100, FMR1000 and ZeroFMR) are reported in Table 1. The results show that the proposed strategy can greatly reduce false acceptance rate and then improve the algorithm's performance.

4.2. Overall performance

Firstly, we give the parameters used during the matching process: the sampling interval (10 pixels), the thresholds used in (17) ($\beta_{Thr1} = \pi/6$ and $\beta_{Thr2} = 5\pi/12$), the threshold used in (22) ($\sigma = 1$). And all the parameters used in two databases are exactly the same. To evaluate the overall performance of the proposed algorithm, we have compared four relevant algorithms (A,B,C,D) on the databases of FVC2004 DB1 and FVC2004 DB3. Algorithm A uses the conventional method (15) to calculate matching score. Algorithm B fuses the matching rate score (15) and global similarity (17). Algorithm C fuses the matching rate score (15)

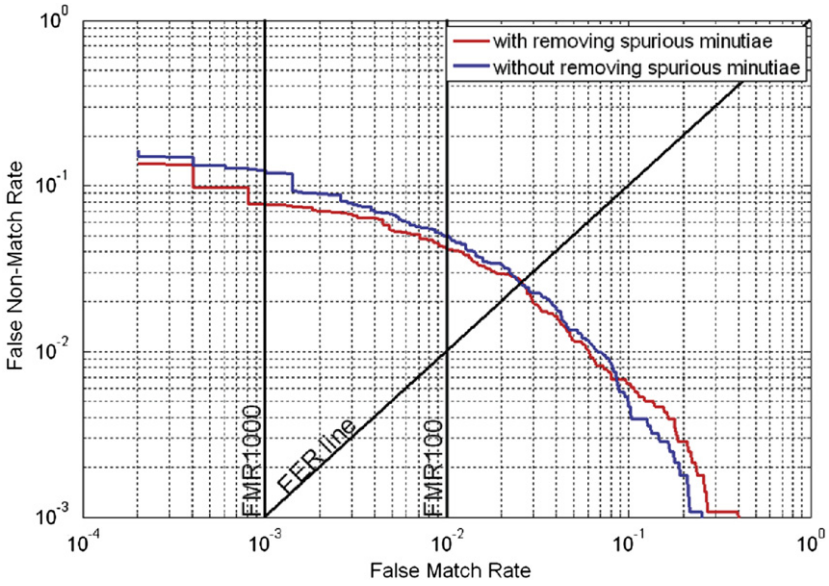

Fig. 6. ROC curves of algorithms with and without removing spurious minutiae.

Table 1
Results of different algorithms.

Methods	EER (%)	FMR100 (%)	FMR1000 (%)	ZeroFMR (%)
Without removing spurious minutiae	2.56	5.18	13.21	16.18
With removing spurious minutiae	2.59	4.18	7.75	13.61

and ridge compatibility (22). And algorithm D is the proposed approach that combined three similarity measures by product rule. To valid the proposed algorithm, we also compare our algorithm with other recent published fingerprint matching results. Algorithms E and F are both from Wang et al. (2007). The difference lies that Algorithm E only uses OrientationCode while Algorithm F fuses OrientationCode and PolyLine, where PolyLine is the latest feature of ridge. Algorithm G is from Tong et al. (2008).

The ROC curves of four algorithms (Algorithms A–D) are plotted in Fig. 7(a) and (b). The algorithm performance indices (EER, FMR100, FMR1000 and ZeroFMR) of above seven algorithms are reported in Tables 2 and 3. From ROC curves, we can see that algorithm D always obtains the best results, which proves that incorporating finger placement direction and ridge compatibility can effectively reduce false match rate (FMR) and then improve the matching accuracy. More details are analyzed as follows:

(1) Adopting the finger placement direction leads very good matching performance on FVC2004 DB3. In this database, these fingerprints were acquired through the thermal sweep sensor "FingerChip FCD4B14CB" by Atmel. The size of the image is 300×480 pixels with a resolution of 512 dpi. Hence, most of the fingerprints are slightness and we can obtain their finger placement directions accurately. Therefore, the FMRs associated with the global feature (Algorithms B and D) drop down quickly with respect to their FNMRs. We take the comparison in Fig. 1 as an example. The matching score of these two fingerprints resulted from Algorithm A is 0.0406 while the matching score threshold at EER point is about 0.0384. With the global feature (Algorithm B), the matching score of these two fingerprints is 0.0234 while the matching score threshold at EER point is about 0.0366. The EER of Algorithm B on FVC2004DB3 is dropped to 1.91% from 2.59% resulted from Algorithm A.

(2) The ridge compatibility significantly improves the matching performance on FVC2004 DB1 and FVC2004 DB3. The EERs of Algorithms A and C on FVC2004 DB1 and DB3 are 3.99% vs. 3.40% and 2.59% vs. 1.96%, with average 0.61% decrease. In Algorithm F (Wang et al., 2007) the fusion method that fuses OrientationCodes and PolyLines performs a little better than only OrientationCodes-based method (Algorithm E). On FVC2004 DB1 and DB3, the differences between the EERs of the fusion method and OrientationCodes-based method are within 0.2%, which indicates PolyLines is hard to improve matching performance largely on large-distorted fingerprints. Compared with PolyLines, our SVD-based ridge compatibility seems much more robust to nonlinear distortion. The phenomena can be interpreted from their viewpoints of representing feature. In the conventional ridge-based methods, one or several features (Jain et al., 1997; He et al., 2003; Wang et al., 2007) are calculated for each sampling point and the differences between the matched sampling points are utilized to calculate ridge similarity. However, the number of ridge sampling points may vary because of noise and the features of the sampling point far away from minutia may possess large variation because of distortion. It is hard to select parameters to measure the similarity between ridges. In the proposed algorithm, ridge similarity is a function of the ridge compatibility which is based on singular value decomposition of affine matrix. There are mainly two advantages of the ridge compatibility: (1) Affine matrix has and only has two singular values, and both of them are expected to be 1 for genuine matches. Hence it is easy to select parameters to measure ridge similarity. (2) The more the number of the sampling point is, the more accurate the affine matrix is. The singular values have small variation even when large distortion exists. Fig. 8 shows the probability distribution of the value of *RC* in genuine match and imposter match on DB1 and DB3. From Fig. 8, we find that *RC* in genuine match follows exponent distribution and it has very good classification performance. The average value of *RC* of genuine

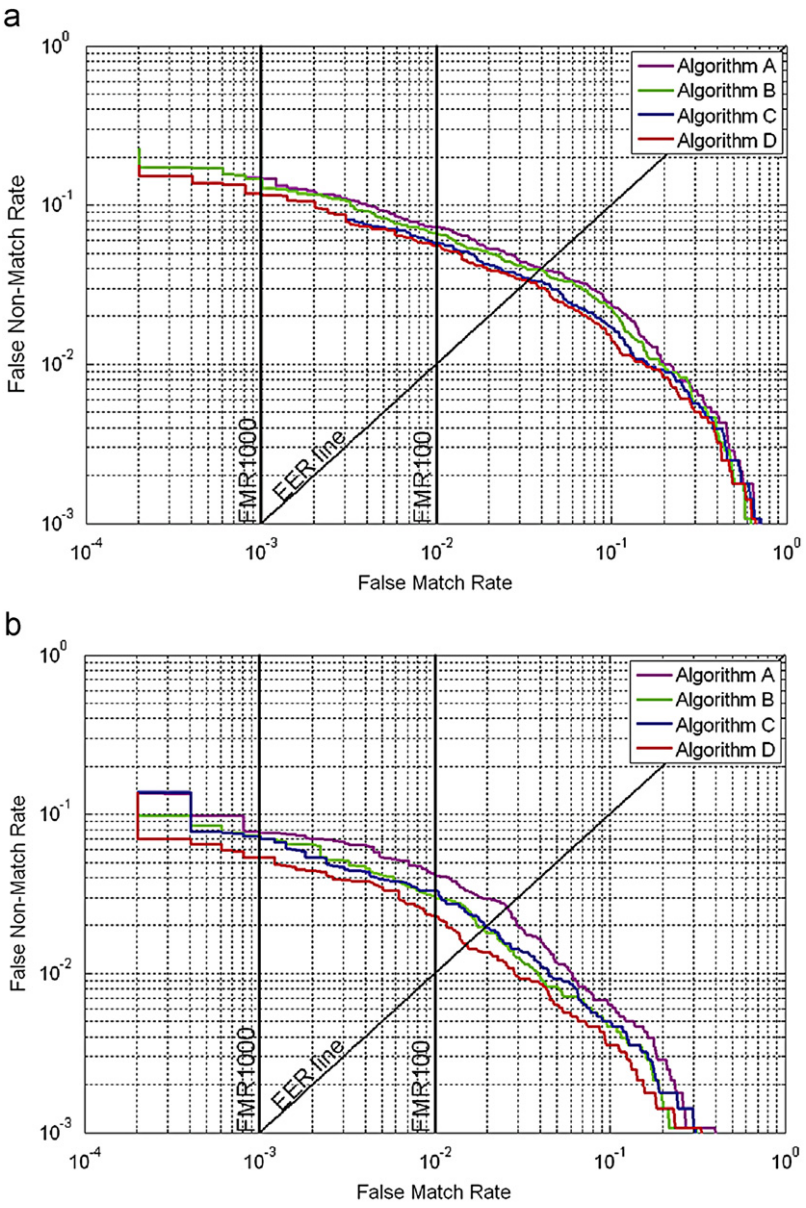

Fig. 7. ROC curves of different algorithms on FVC2004. (a) DB1, (b) DB3.

Table 2
Results of different algorithms over FVC2004 DB1.

Algorithm	EER (%)	FMR100 (%)	FMR1000 (%)	ZeroFMR (%)
A	3.99	7.25	14.79	22.68
B	3.93	6.61	14.68	22.68
C	3.40	5.82	11.79	17.89
D	**3.35**	**5.57**	**11.79**	**17.89**
E	7.68	13.46	27.11	–
F	7.49	14.5	24.29	–
G	7.47	–	–	–

Table 3
Results of different algorithms over FVC2004 DB3.

Algorithm	EER (%)	FMR100 (%)	FMR1000 (%)	ZeroFMR (%)
A	2.59	4.18	7.75	13.61
B	1.91	3.04	7.36	13.61
C	1.96	3.29	7.29	13.75
D	**1.49**	**2.32**	**5.39**	**13.75**
E	2.97	5.64	11	–
F	2.83	4.36	9.46	–
G	1.89	–	–	–

matches for DB1 and DB3 are 0.607 and 0.431, respectively. This difference may indicate that the distortion of DB1 is larger than DB3.

(3) The global feature is determined by the finger placement. It does not have any relation with the patterns of ridges and valleys on the skin surface. Therefore, the global feature and the ridge compatibility can be considered to be independent of each other. From the results on the two databases, the decrease of EER of Algorithm D is approximately equal to the sum of those of Algorithms B and C. On FVC2004 DB3, the fusion algorithm also decreases the EER greatly. The EERs of the fused strategy on DB1 and DB3 are 3.35% and 1.49%, respectively. Both of them are lower than the methods proposed by Wang et al. (2007) and Tong et al. (2008). Moreover, the proposed algorithm can obtain the third place in FVC2004 (2004) ranked by EER.

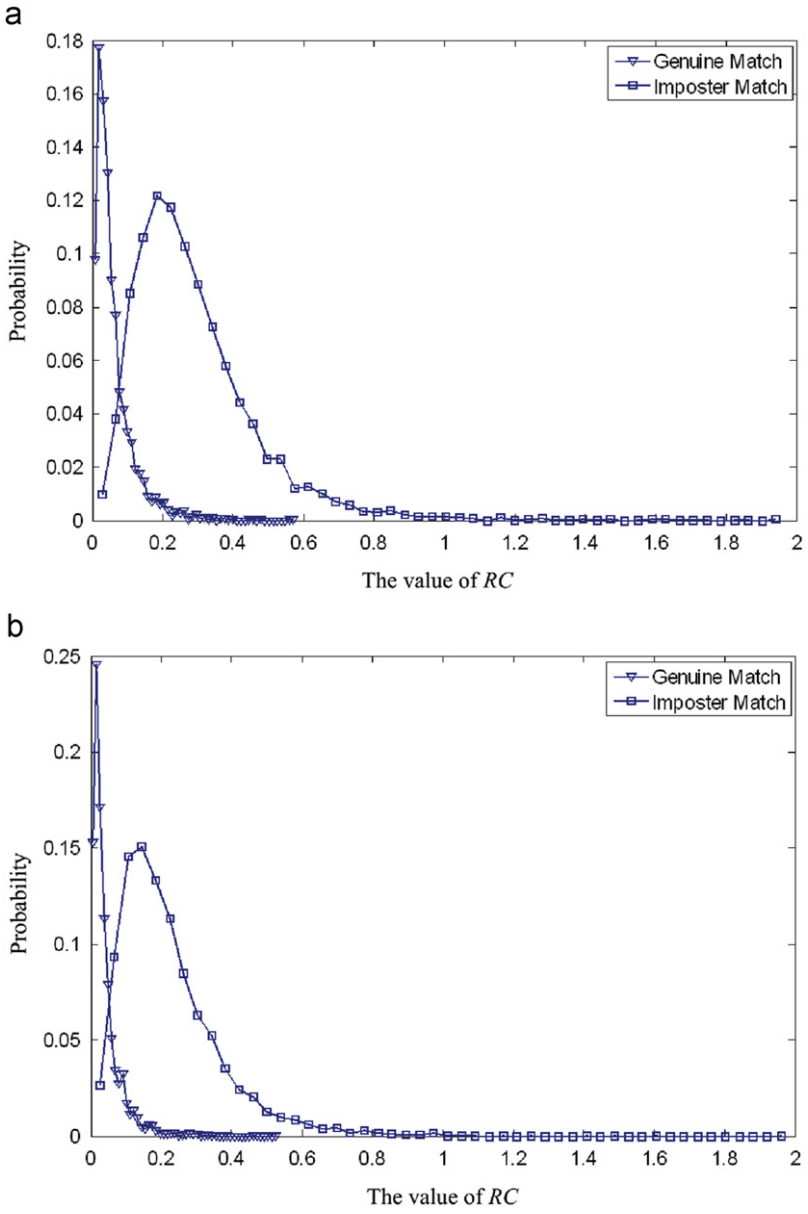

Fig. 8. Probability distribution of ridge compatibility on FVC2004 DB1. The part, where the value of *RC* is larger than 2, is cut off for better comparison. (a) DB1, (b) DB3.

(4) All the experiments are conducted on the same PC with Intel Pentium 4 processor 3.4 GHz under Windows XP professional operating system. All the fingerprint matching algorithms are implemented using the C++ language. The average matching times of Algorithms A, B, C and D on FVC2004 DB1 are 26.9, 27.0, 30.0 and 30.1 ms, respectively. The average matching times of that four algorithms on FVC2004 DB3 are 31.6, 31.9, 35.1 and 35.2 ms, respectively. Local minutiae similarity calculation is a time-consuming process and most of the matching are spent on it. The average increase of matching time between Algorithms B and A is 0.2 ms. Ridge compatibility calculation involves least square estimation and SVD. Therefore, it is much more time-consuming than global similarity and its matching time increases average 3.3 ms.

5. Conclusion and future work

In this paper, we propose an effective approach to remove spurious minutiae close to creases and introduce a global feature called finger placement direction. Both of these methods are designed to directly reduce false acceptance rate. Ridge compatibility is measured by the singular values of the affine matrix which is estimated by the ridges associated with the matched minutiae. Experimental results indicate that the preprocessing approach can remove most spurious minutiae resulted from creases, and the two features are effective to improve the matching performance. The equal error rates reach 3.35% and 1.49% on DB1 and DB3, respectively, and both of them can rank the third place in FVC2004.

However, the FMR1000 and ZeroFMR of the proposed algorithm are still high. We will resort to other features especially global features (such as singular point and class information) to reduce these indices. The proposed algorithm can still not deal with large-distorted fingerprints because it is very difficult to establish minutiae correspondences between two fingerprints with large nonlinear distortion by considering only rotation and translation transformation. Future works may try to find a novel and effective approach to solve this problem.

Acknowledgments

This paper is supported by the Project of National Natural Science Foundation of China under Grant nos. 60875018 and 60621001, National High Technology Research and Development Program of China under Grant no. 2008AA01Z411, Chinese Academy of Sciences Hundred Talents Program, Beijing Natural Science Foundation under Grant no. 4091004, Scientific Databases Program of the Chinese Academy of Sciences during the 11th Five-Year Plan Period under Grant no. INFO-115-C01-SDB4-30.

References

Bazen A, Gerez S. Systematic methods for the computation of the directional fields and singular points of fingerprints. IEEE Transactions on Pattern Analysis and Machine Intelligence 2002;24(7):905–19.

Bazen A, Gerez S. Fingerprint matching by thin-plate spline modelling of elastic deformations. Pattern Recognition 2003;36(8):1859–67.

Cao K, Yang X, Tian J, Zhang Y, Li P, Tao X. Fingerprint matching based on neighboring information and penalized logistic regression. In: Advances in biometrics, third international conference, ICB 2009. p. 617–26.

Chen X, Tian J, Yang X. A new algorithm for distorted fingerprints matching based on normalized fuzzy similarity measure. IEEE Transactions on Image Processing 2006;15(3):767–76.

Chen X, Tian J, Cheng J, Yang X. Segmentation of fingerprint images using linear classifier. EURASIP 2004;4:480–94.

Cormen TH, Leiserson CE, Rivest RL, Stein C. Introduction to algorithms, 2nd ed. Cambridge, New York: MIT Press, McGraw-Hill; 2001. [Chapter 21].

Feng J. Combining minutiae descriptors for fingerprint matching. Pattern Recognition 2008;41(1):342–52.

Freemam H, Shapira R. Determining the minimum-area encasing rectangle for an arbitrary closed curve. Communications of the ACM archive 1975;18(7):409–13.

FVC2002 〈http://bias.csr.unibo.it/fvc2002/〉, 2002.

FVC2004 〈http://bias.csr.unibo.it/fvc2004/〉, 2004.

Graham RL. An efficient algorithm for determining the convex hull of a finite planar set. Information Processing Letters 1972;26(3):132–3.

Gu J, Zhou J, Yang C. Fingerprint recognition by combining global structure and local cues. IEEE Transactions on Image Processing 2006;15(7):1952–64.

He Y, Tian J, Li L, Chen H, Yang X. Fingerprint matching based on global comprehensive similarity. IEEE Transactions on Pattern Analysis and Machine Intelligence 2006;28(6):850–62.

He Y, Tian J, Luo X, Zhang T. Image enhancement and minutiae matching in fingerprint verification. Pattern Recognition Letters 2003;24(9–10):1349–60.

Holland P, Welsch R. Robust regression using iteratively reweighted least-squares. Communications in Statistics Theory and Methods 1977;A6:813–27.

Hong L, Wan Y, Jain A. Fingerprint image enhancement: algorithm and performance evaluation. IEEE Transactions on Pattern Analysis and Machine Intelligence 1998;20(8):777–89.

Jain A, Hong L, Bolle R. On-line fingerprint verification. IEEE Transactions on Pattern Analysis and Machine Intelligence 1997;19:302–14.

Jea TY, Govindaraju V. A minutia-based partial fingerprint recognition system. Pattern Recognition 2005;38:1672–84.

Jiang X, Yau WY. Fingerprint minutiae matching based on the local and global structures. In: Proceedings of the 15th international conference on pattern recognition, vol. 2, 2000. p. 1038–41.

Luo X, Tian J, Wu Y. A minutia matching algorithm in fingerprint verification. In: Proceedings of the 15th international conference on pattern recognition, vol IV, 2000. p. 833–6.

Maio D, Maltoni D. A structural approach to fingerprint classification. In: Proceedings of the 13th international conference on pattern recognition, 1996.

Maltoni D, Maio D, Jain A, Prabhakar S. Handbook of fingerprint recognition, 2nd ed. London: Springer; 2009.

Qi J, Yang S, Wang Y. Fingerprint matching combining the global orientation field with minutia. Pattern Recognition Letters 2005;26:2424–30.

Ratha N, Pandit V, Bolle R, Vaish V. Robust fingerprint authentication using local structural similarity. In: Fifth IEEE workshop on applications of computer vision, 2000. p. 29–34.

Sha L, Zhao F, Tang X. Minutiae-based fingerprint matching using subset combination. In: Proceedings of the 18th international conference on pattern recognition, vol. IV, 2006. p. 566–9.

Sheng W, Howells G, Fairhurst M, Deravi F. A memetic fingerprint matching algorithm. IEEE Transactions on Information Forensics and Security 2007;2(3):402–12.

Tico M, Kuosmanen P. Fingerprint matching using an orientation-based minutia descriptor. IEEE Transactions on Pattern Analysis and Machine Intelligence 2003;25(8):1009–14.

Tong X, Huang J, Tang X, Shi D. Fingerprint minutiae matching using the adjacent feature vector. Pattern Recognition Letters 2005;26(9):1337–45.

Tong X, Liu S, Huang J, Tang X. Local relative location error descriptor-based fingerprint minutiae matching. Pattern Recognition Letters 2008;9:286–94.

Wang X, Li J, Niu Y. Fingerprint matching using orientationcodes and polylines. Pattern Recognition 2007;40(11):3164–77.

Yager N, Amin A. Fingerprint verification based on minutiae features: a review. Pattern Analysis and Applications 2004;7:94–113.